PHYSICAL REVIEW B **102**, 155204 (2020)

Large substitutional impurity isotope shift in infrared spectra of boron-doped diamond

D. D. Prikhodko,[1,2,*] S. G. Pavlov,[3] S. A. Tarelkin,[2,4,5] V. S. Bormashov,[5] M. S. Kuznetsov,[2] S. A. Terentiev,[2]
S. A. Nosukhin,[2] S. Yu. Troschiev,[2,5] H.-W. Hübers,[3,6] and V. D. Blank[1,2,4]
[1] *Moscow Institute of Physics and Technology, 141701 Dolgoprudny, Moscow Region, Russia*
[2] *Technological Institute for Superhard and Novel Carbon Materials (TISNCM), 108840 Troitsk, Moscow, Russia*
[3] *Institute of Optical Sensor Systems, German Aerospace Center (DLR), 12489 Berlin, Germany*
[4] *National University of Science and Technology MISiS, 119049 Moscow, Russia*
[5] *The All-Russian Research Institute for Optical and Physical Measurements, 119361 Moscow, Russia*
[6] *Department of Physics, Humboldt-Universität zu Berlin, 12489 Berlin, Germany*

(Received 14 November 2019; revised 25 September 2020; accepted 25 September 2020; published 16 October 2020)

Isotopic enrichment offers cutting-edge properties of materials. In semiconductors, contributions to physical properties from different isotopes can be routinely and precisely examined by different optical techniques down to a very low relative atomic content in the crystal lattice. In the case of impurity centers this can be as low as a few ppm. We report the splitting of infrared absorption lines caused by the isotopic content of boron acceptors embedded in semiconducting diamond. A blueshift as large as 0.2% of the intracenter transition energy of ^{10}B relative to the ^{11}B transitions has been observed in diamond with natural boron abundance. This is a large isotopic shift for hydrogenlike substitutional impurity centers in semiconductors. Also, a much smaller ($\sim$0.01%) redshift of ^{11}B transitions in diamond doped with natural boron has been observed relative to the ^{11}B transitions in diamond doped by enriched ^{11}B (up to 99%).

DOI: 10.1103/PhysRevB.102.155204

I. INTRODUCTION

The isotopic shifts of impurity atoms in the lattices of semiconductors are well known. They can be expressed by phonon modes with characteristic frequencies proportional to the ratio of the square root of the isotopic masses [1]. Usually these frequency shifts are sufficiently large to be spectrally resolved by Raman spectroscopy or by infrared absorption spectroscopy.

Isotopic disorder of elements affects the optical properties of semiconductors through electron-phonon interaction and volume changes. Both depend on the average isotopic mass [2] and the random distribution of the isotopes [3] in the host lattice. This results in changes of band gaps and phonon spectra. Also the impurity spectra change: the impurity transitions are splitted and broadened. In doped silicon, the presence of three different lattice isotopes broadens the impurity spectral lines ($\sim$25 μeV) due to the random distribution of the silicon atoms with different masses [4]. In ^{13}C-enriched boron-doped diamond, a gradual shift (from 3.1 to 11.8 cm^{-1}) of the whole impurity spectrum occurs as compared to ^{12}C-enriched crystals [5]. However, the influence of ^{13}C on the line shape and linewidth of boron intracenter transitions with natural carbon isotopic content has not been determined because of the weak effect by the low abundance of the isotope (1.1%).

The shifts caused by isotopic disorder of impurity centers with much lower concentration are commonly assigned to the weak dependence of the center's ground-state energy on the mass of the impurity atom, assigned to existence of local vibrational modes (LVM) [6,7]. The impurity-bound LVMs differ from phonon modes of the lattice (e.g., optical phonons with energy $\hbar\Omega_{\text{OP}}$) in energy ($\hbar\Omega_{\text{LVM}}$, Ω_{LVM} is the frequency of the LVM) and in localization [$\Lambda_{\text{LVM}i} = (\hbar/M_i\Omega_{\text{LVM}i})^{1/2}$] for a specific defect with a mass M_i. Thus, the stronger the localization of a LVM at a lattice defect and the stronger the defect is bound to the lattice, the weaker is the isotopic shift and the more challenging is its determination. In general, these are hardly accessed by low-temperature Raman or absorption spectroscopy even in heavily doped samples, when isotopic shifts of impurity electronic states are spectrally unresolved because of concentration broadening of their lines.

Infrared absorption or photoluminescence spectroscopy is a powerful technique if the isotopic shifts are large, i.e., larger than 0.01% of the corresponding transition energy $\hbar\omega$ [4,8–10]. Impurity isotope shifts are often used to derive the energy of LVM of a defect [1,7] or to prove the type of color center in solids [6,8–10]. Large shifts of the ground-state energy, about several hundred μeV ($\sim$0.1% of ionization energy E_i), were observed for deep isoelectronic traps [11,12] or for deep donors [9] and acceptors in semiconductors [10]. So far the reported values of isotopic splitting in impurity spectra of shallow hydrogenlike donors or acceptors are very small [4,6,13], on the order of $\sim$10 μeV, and were hardly observed by spectroscopy because of various line broadenings. For example, isotope splitting induced by boron, which is 0.15 cm^{-1} (19 μeV, 0.05% of the boron transition energy $\hbar\omega$), was observed in low-temperature infrared absorption spectra only in isotopically purified silicon [4].

---

[*] prikhodko.dd@phystech.edu

Until now, there is no general theory of impurity isotope shifts in semiconductors. The commonly accepted physical mechanism of isotopic impurity shift is due to LVM-induced relative changes of the zero-point energy caused by the different impurity mass and the softening of lattice oscillation modes. In a simple diatomic lattice model, with impurity isotope centers of a mass M_i $(i = 1, 2)$ attached to a host atom of mass M with coupling-force constants k_i, the ratio of characteristic energies of different isotopic oscillators is [1]

$$\frac{\hbar\omega_1}{\hbar\omega_2} = \frac{k_1}{k_2}\left[\frac{\left(1 + x\frac{M}{M_1}\right)}{\left(1 + x\frac{M}{M_2}\right)}\right]^{1/2}, \qquad (1)$$

where the empirical factor x accounts for the vibrations of other host atoms. Obviously two major contributions to isotopic energy shifts, ΔE_i, are local changes of the coupling forces between impurities and host atoms ($\sim k_i$) as well as atomic mass differences ($\Delta M_{12} = M_1 - M_2$). The first contribution, $\Delta E_i/E_i \sim \gamma(M/M_i)^{1/2}\Delta M_i/M_i$, called "phonon softening" and expressed by the empirical factor γ, has been considered in the zero-phonon isotopic shift approach developed by Heine and Henry [14]. The authors have shown that their formalism allows explaining the major trends of the large, experimentally observed isotopic shifts of different impurities in GaP (ΔE_i up to 0.8 meV, 0.3% of transition energy). This includes substitutional donor and acceptor centers with an isotope mass difference of $\Delta M_{12} = 2$ amu, revealing relative shifts $\Delta E_i/E_i$ of 0.17% for acceptors and 0.06% for donors. Contributions to the energies of impurity states through changes of the long-distance impurity potential and through the short-distance central cell correction (ccc) have been considered by Kogan [6]. The latter are caused by changes of the oscillation magnitudes, Λ_{LVM}, of atoms with different masses M_i, $\Delta E_i/E_i \sim (\Lambda_{\mathrm{LVM}}/l)^2$, where l is the effective Bohr radius (long-distance corrections) or characteristic bond length (ccc). Such an approach provided the estimates of isotopic shifts of the impurity ground-state energy $\Delta E_i \sim {\Lambda_{\mathrm{LVM}}}^2$ on the order of a few tens of μeV ($\Delta E_i/E_i$ up to ~0.3%), similar to those observed when hydrogen is replaced by deuterium in impurity complexes of germanium [8].

In general, interstitial impurities and complexes reveal larger isotopic shifts [14,15]. Substitutional hydrogenlike impurity centers in elemental semiconductors, having strong covalent bonds to the host lattice atoms with much smaller Λ_{LVM} compared with interstitial impurities, reveal smaller isotopic shifts.

The masses of stable isotopes of boron, as the lightest substitutional hydrogenlike dopant in elemental semiconductors, have large relative differences ΔM_{12}, ^{10}B: 10.0129 amu and ^{11}B: 11.0093 amu. This large $M_{11} - M_{10} = 0.1M_{10}$ difference together with the small mass of carbon in the diamond lattice, $M = 12.0096$ amu for natural diamond with 98.9% of ^{12}C, makes the largest contribution in the mass-related factor of the isotopic shift [Eq. (1)] in the virtual lattice. Additionally, the boron acceptor in diamond has a large ionization energy E_i. The reported values range from 368.5 meV [16] to 382 meV [17]. This enables, as shown here experimentally, to access the isotopic composition of boron in diamond by infrared absorption spectroscopy. By comparison of low-temperature absorption spectra of a diamond sample with natural boron content (20% of ^{10}B and 80% of ^{11}B isotopes) and ^{11}B-enriched (up to 99%) diamonds, grown by the high-pressure high-temperature technique, it is possible to distinguish the intracenter transitions of ^{10}B and ^{11}B isotopes. We have found that the isotopic spectral lines of the closest ^{10}B and ^{11}B boron intracenter transitions are separated by 0.72 ± 0.03 meV (~0.2% of boron ionization energy). The blueshift of the ^{10}B ground-state energy relative to the ^{11}B ground-state energy fits to the regularly observed trend for the light atoms. This shift results presumably from the chemical shifts of the boron ground state through interaction with a local vibration mode of boron in diamond. It is among the largest isotopic shifts for a hydrogenlike substitutional impurity in a semiconductor ever reported.

II. EXPERIMENT

A. Sample preparation and characterization

In this work, we used single-crystal boron-doped diamonds grown in the Technological Institute for Superhard and Novel Carbon Materials by the temperature gradient method at high-pressure, high-temperature conditions with simultaneous doping of diamond by boron from the melt. More details of the growth process can be found elsewhere [18]. Two types of boron sources were used for doping: standard amorphous boron powder with natural isotopic content (80% ^{11}B +20% ^{10}B) and boron oxide B_2O_3 enriched up to 99% with ^{11}B.

The (001)-oriented plates were laser cut from the top (opposite side of the seed) of the grown diamonds as shown in Fig. 1. Then the plates were double-side polished with a wedge of ~1° to suppress optical interference in the samples.

A (001) growth sector of a diamond crystal is most preferable for spectroscopy as it has the most uniform dopant distribution and the lowest density of crystal defects. We used UV-excited photoluminescence images of the plates, taken with a DiamondView™ instrument, in order to distinguish different growth sectors as shown in Fig. 1(b). Individual metal shadow masks for each sample were used to select the area opened to transmitted light.

The boron concentration was determined from the absorption spectra at 300 K using a calibration based on the integrated absorption of the boron absorption band at 347.3 meV [16]. Since the growth process causes an unavoidable capture of residual nitrogen in the crystal, which occurs as a deep donor with a concentration $<10^{15}$ cm^{-3}, the determined boron concentration refers always to uncompensated acceptor centers. The uncompensated boron concentration in our set of samples varies from $\sim 7 \times 10^{15}$ cm^{-3} to $\sim 3 \times 10^{17}$ cm^{-3} (~40 ppb–2 ppm relative to the carbon host atoms). For comparison of the infrared spectra, we have chosen two pairs of samples with similar ^{11}B concentration and different isotope content, namely the samples BDD-07 and BDD-1-8-001-1 with natural boron (the total uncompensated boron ^{11}B + ^{10}B concentration is $\sim 7.1 \times 10^{16}$ cm^{-3} and $\sim 5.0 \times 10^{15}$ cm^{-3}, respectively) and the samples 07mg_1 and 02mg_1 with enriched ^{11}B ($\sim 6.5 \times 10^{16}$ cm^{-3} and $\sim 1.8 \times 10^{16}$ cm^{-3}, respectively).

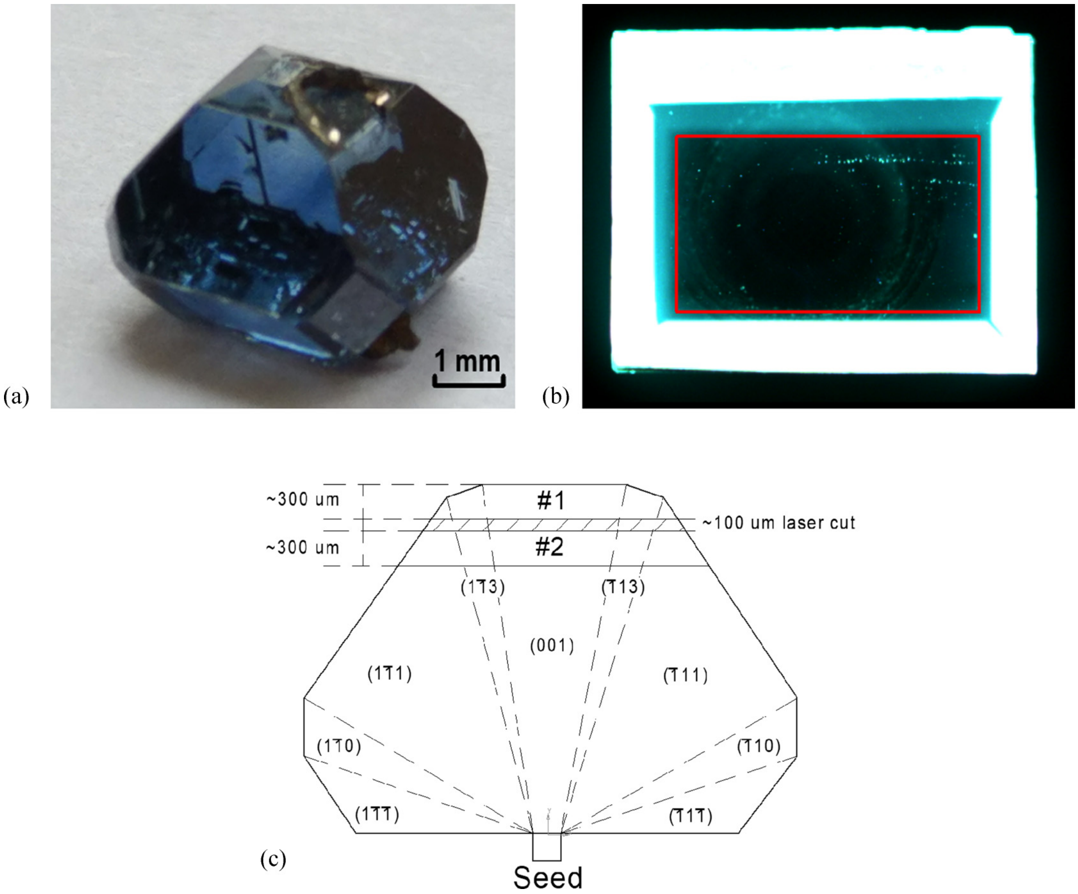

FIG. 1. Sketch of a typical boron-doped diamond grown by the high-pressure high-temperature technique: (a) photo of an as-grown crystal (sample 07mg_B2O3); (b) example of a UV-excited photoluminescence image of the sample 07mg_1 with three growth sectors: (001) – dark area in the center, four (113) family sectors – light blue area in the middle, and four (111) family sectors – bright "white" area outside; (c) 2D projection of a grown crystal in the growth direction showing two 300-μm cut plates #1 and #2. In the infrared absorption spectroscopy experiments, only the central part marked by a red frame is open while the rest of the crystal is covered by a mask.

B. Infrared spectroscopy

To obtain high-resolution infrared spectra we used a Bruker Vertex 80v$^{\mathrm{TM}}$ Fourier-transform spectrometer. It was equipped with a Janis helium flow cryostat to achieve temperatures down to about 5 K, as measured by a thermosensor on its cold finger. The samples were attached to the cold finger of the cryostat using a thermally conductive silver paint. Each sample was covered by a mask with a central rectangular opening [see Fig. 1(b)]. We used the standard components of the spectrometer for the midinfrared wavelength range: a globar light source, a coated KBr beam splitter, and a liquid-nitrogen-cooled mercury-cadmium-tellurium detector. The resolution of the spectrometer was probed in order to estimate the optimal value for the best signal-to-noise ratio and for most of measurements was 0.03 meV ($0.25\,\mathrm{cm}^{-1}$). The absorption spectra were taken in the temperature range from 5 to 300 K. Because of the different light throughput determined by the individual mask area, the transmission spectra were normalized by a common spectral feature: the two-phonon band in the range from 270 to 330 meV taken for an undoped IIa diamond.

III. RESULTS AND DISCUSSION

The main feature of the spectra (Fig. 2) is the different number of boron related lines in crystals doped with natural boron ($^{10}\mathrm{B} + {}^{11}\mathrm{B}$) and crystals doped with isotopically enriched boron ($^{11}\mathrm{B}$). $^{10}\mathrm{B}$ lines appear as excess acceptor transitions. Some of them are accurately spectrally resolved and the transition frequency is unambiguously assigned (Table I). The determination of weaker lines and those on the wings of close-by, strong transitions is less accurate and precise. The isotopes $^{10}\mathrm{B}$ and $^{11}\mathrm{B}$ appear in the absorption spectra (Fig. 2) as "doublet" set with a constant energy interval of $0.72 \pm 0.03\,\mathrm{meV}$ for the most intense and clearly resolved boron lines in the spectra of a sample with natural boron isotopic composition. These doublets merge to a "single" line set in the spectra of the $^{11}\mathrm{B}$ enriched sample. The line intensity ratio in these doublets reflects the $^{11}\mathrm{B}/^{10}\mathrm{B}$ natural abundance ratio of ∼80/20. The intensity ratio of the doublets does not depend on temperature, unlike additional thermally induced 2-meV redshifted doublets, which arise due to transitions from the split ground state. The weaker line in all doublets has the larger photon energy. This fact

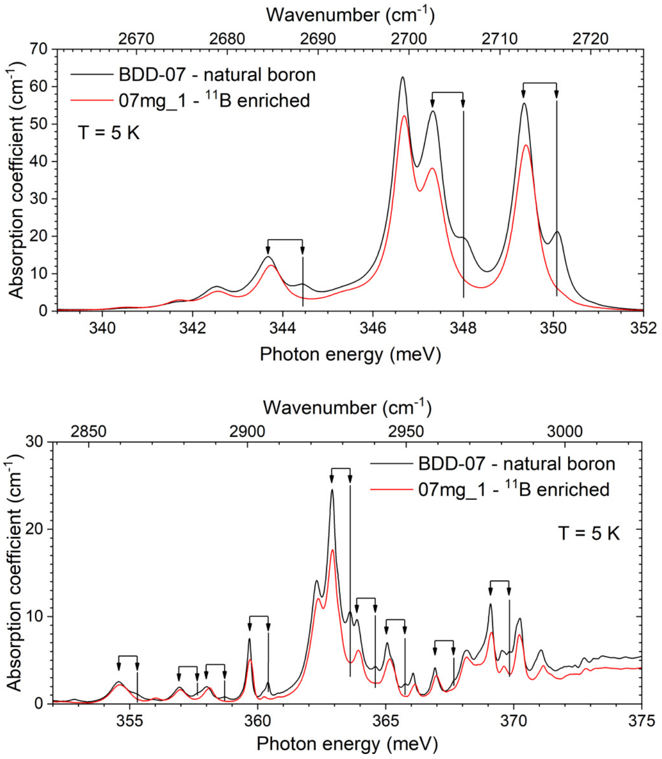

FIG. 2. IR absorption spectra of two diamond samples doped with boron with different isotopic composition. The sample BDD-07 (black line) is doped with natural boron (80% ^{11}B and 20% ^{10}B) while the sample 07mg_1 (red line) is doped with isotopically enriched ^{11}B. Spectra are taken at 5 K. Large isotopic doublets (corresponding to ^{11}B and ^{10}B) are marked by pairs of black arrows.

matches the general rule that optical intracenter transitions of lighter impurity isotopes have higher energies, i.e., a larger chemical shift [6,14]. We interpret the observed structure as isotope splittings of impurity transitions of ^{10}B and ^{11}B in diamond. To confirm this assumption, we compared the infrared absorption spectra of diamonds doped with boron with different isotopic composition (see Fig. 2). The weak, high-energy component of each doublet disappears in the spectra of the 07mg_1 sample doped with isotopically enriched boron. The same isotopic shift is observed in the infrared spectra of lower-doped samples pair, BDD-1-8-001-1 and 02mg_1.

Our estimates of the isotope shift made in the frame of the models proposed by Kogan [6] or Heine [14], and using the best-known parameters for a boron-doped diamond adapted from these publications, do not yield a close value for the shift observed in our spectra. The "mode softening" model [14] gives a value of $\Delta E_i \sim 3.5\,\text{meV}$, while the mass correction in the energy of the impurity ground state [6] gives a value of only $\Delta E_i \sim 7\,\mu\text{eV}$. Although the discrepancy to the measured isotope shift can be partly explained by poor knowledge of the Ω_{LVM} of boron in diamond and softening constants for diamond, one can estimate the characteristic localization of the LVM in the high limit as $\Lambda_{\text{LVM}} = (\hbar/M_{11}\Omega_{\text{LVM}})^{1/2}$ (Ref. [6]), assuming a lattice atom (^{12}C) is replaced by a lighter impurity (^{11}B). This leads to a LVM frequency larger than the maximal phonon frequency in the undisturbed lattice, i.e., the zone-centered optical phonon in diamond ($\hbar\Omega_{\text{OP}} = 165\,\text{meV}$): $\Omega_{\text{LVM}} > \Omega_{\text{OP}}$. Such an estimate, $\Lambda_{\text{LVM}} < 5\,\text{pm}$, shows that the LVM acts on a scale less than the characteristic bond lengths. Such strongly localized interactions cannot be properly introduced as first-order corrections in the impurity chemical shift, as proposed in the discussed models. Instead, the interaction with a LVM must be used for the calculation of the energy spectrum of an impurity from first principles. Thus, we assume that the cited approaches lose their validity for strongly localized LVM on an impurity center, that is the case

TABLE I. Energies of boron isotope infrared transitions (in meV) as determined from their infrared absorption spectra of samples with similar boron concentrations (in paired columns). All transition energies were determined from the peak of the absorption line with an accuracy of about 0.004 meV. The isotope shift was calculated as the difference between ^{10}B and ^{11}B transitions energies of the same natural boron-doped sample (C:^{10}B + ^{11}B), while ^{11}B lines were checked from the comparison with the C:^{11}B sample of similar ^{11}B concentration. Only the ^{10}B lines with relatively high intensity, enabling accurate determination of the line center, are used for calculation of the mean value of the shift.

BDD-07 natural 7.1×10^{16} cm^{-3}			07mg_1 enriched 6.5×10^{16} cm^{-3}	BDD-1-8-001-1 natural 5.0×10^{15} cm^{-3}			02mg_1 enriched 1.8×10^{16} cm^{-3}
^{11}B	^{10}B	Shift	^{11}B	^{11}B	^{10}B	Shift	^{11}B
343.663	344.396	0.733	343.732	343.693	344.417	0.724	343.704
346.668	347.3		346.722	346.691	347.3		346.725
347.271	348.0		347.277	347.286	348.0		347.266
349.357	350.054	0.697	349.363	349.363	350.061	0.698	349.367
354.600	355.3		354.645				354.603
356.962	357.7		357.008	356.944			357.000
357.977	358.7		358.072	358.044			358.084
359.653	360.381	0.728	359.686	359.659	360.382	0.723	359.699
362.336	363.0		362.386	362.321	363.0		362.343
362.897	363.586	0.689	362.889	362.898	363.645	0.747	362.939
363.833	364.573	0.740	363.914				363.904
365.071	365.8		365.147				365.092
366.925	367.7		367.004				366.983
369.060	369.8		369.087	369.078	369.8		369.112

of strongly bounded substitutional centers in semiconductors with a cubic-type lattice.

A significant impact could come from the fact that the boron absorption lines are close to the two-phonon band of the host lattice and the model does not take into account resonant effects, neither with respect to the host phonons nor to the LVMs. It should be noted that strong interactions of boron states with the host lattice phonons are likely to exist, because they explain also another experimental finding, namely the ultrafast nonradiative decay of excited boron states in diamond [19].

Another weak feature can be found by a systematic analysis of the relative line positions of ^{11}B in the samples doped by natural boron and the samples doped by enriched ^{11}B. A comparison of the ^{11}B transition energies in the sample BDD-07 with those in the sample 07mg_1 indicates a regular slight redshift of 0.04 ± 0.03 meV in the natural boron-doped sample. In the case of the samples BDD-1-8-001-1 and 02mg_1 with lower boron concentrations, the mean shift of the ^{11}B transition energy is less ($\sim$0.02 meV). Such a shift cannot be related to those caused by interaction with a LVM. Considering that the LVM acts on a scale less than the characteristic bond lengths (1.54 nm for C–C or 1.56 nm for C–B), it does not extend to the scale, characteristic for the interacting ^{10}B and ^{11}B centers, whose mean spatial separation is estimated to be on the order of 10 nm in the samples. An estimate based on the orbitals of the excited state, in which the mentioned boron intracenter transitions terminate, yields a value of 4.6 nm for the doubled radius, which is on the same order as the boron intercenter distances in diamond. We suppose that the observed ^{11}B shift can be caused by different interaction of ^{11}B atoms with the next closest impurity center, ^{11}B or ^{10}B, due to overlapping of their state orbitals.

IV. CONCLUSIONS

The isotopic shifts related to the impurity isotope content of boron in diamonds grown by the high-pressure high-temperature technique have been derived from infrared absorption spectra. The blueshift of intracenter ^{10}B transitions relative to ^{11}B lines indicates a large chemical shift (0.72 ± 0.03 meV) of the ^{10}B isotope ground state relative to the ^{11}B ground state. This is among the largest isotopic shifts (relative shift $\sim$0.2%) ever observed for a hydrogenlike substitutional impurity in semiconductors. The shift profits from the large binding energy of boron and the large relative mass difference. A weaker ^{11}B redshift in natural boron-doped diamond is assigned to the regular isotopic disorder of ^{10}B and ^{11}B centers in the diamond lattice caused by a weak, partial overlap of the orbitals of the highly excited boron states.

Isotopically enriched moderately doped diamond samples reveal the undisturbed absorption line intensities, integrals, and linewidths for boron. Therefore, they are very well suited for studying the excited states of the hydrogenlike boron acceptor in diamond.

ACKNOWLEDGMENTS

Diamond samples treatment and characterization in Technological Institute for Superhard and Novel Carbon Materials were funded by the RSF, Project No. 18-72-00232. Spectroscopy experiments in Technological Institute for Superhard and Novel Carbon Materials were funded by RFBR, Project No. 19-32-90189. The authors acknowledge support from the Deutsche Forschungsgemeinschaft (Project No. GZ: HU 848/10-1). Part of this work was carried out using the Shared Use Equipment Center for high–precision measuring in photonics (ckp.vniiofi.ru, VNIIOFI).

---

[1] F. Thompson and R. Nicklin, J. Phys. C: Solid State Phys. **5**, L223 (1972).

[2] A. K. Ramdas, S. Rodriguez, S. Tsoi, and E. E. Haller, Solid State Commun. **133**, 709 (2005).

[3] M. L.W. Thewalt, Solid State Commun. **133**, 715 (2005).

[4] D. Karaiskaj, J. A. H. Stotz, T. Meyer, M. L.W. Thewalt, and M. Cardona, Phys. Rev. Lett. **90**, 186402 (2003).

[5] H. Kim, A. K. Ramdas, S. Rodriguez, and T. R. Anthony, Solid State Commun. **102**, 861 (1997).

[6] S. M. Kogan, Sov. Phys. Semicond. **13**, 1131 (1979).

[7] B. Dischler, *Handbook of Spectral Lines in Diamond* (Springer Berlin, 2012).

[8] E. E. Haller, Phys. Rev. Lett. **40**, 584 (1978).

[9] P. J. Dean, C. H. Henry, and C. J. Frosch, Phys. Rev. **168**, 812 (1968).

[10] P. J. Dean, C. J. Frosch, and C. H. Henry, J. Appl. Phys. **39**, 5631 (1968).

[11] P. J. Dean, Phys. Rev. B **4**, 2596 (1971).

[12] C. H. Henry, P. J. Dean, and J. D. Cuthbert, Phys. Rev. **166**, 754 (1968).

[13] M. Cardona and M. L.W. Thewalt, Rev. Mod. Phys. **77**, 1173 (2005).

[14] V. Heine and C. H. Henry, Phys. Rev. B **11**, 3795 (1975).

[15] M. D. McCluskey, J. Appl. Phys. **87**, 3593 (2000).

[16] A. T. Collins and A. W. S. Williams, J. Phys. C: Solid State Phys. **4**, 1789 (1971).

[17] E. Gheeraert, S. Koizumi, T. Teraji, H. Kanda, and M. Nesládek, Phys. Status Solidi A **174**, 39 (1999).

[18] V. S. Bormashov, S. A. Tarelkin, S. G. Buga, M. S. Kuznetsov, S. A. Terentiev, A. N. Semenov, and V. D. Blank, Diamond Relat. Mater. **35**, 19 (2013).

[19] S. G. Pavlov, S. A. Tarelkin, V. S. Bormashov, N. Stavrias, K. Saeedi, A. F.G. van der Meer, N. A. Bekin, R. Kh. Zhukavin, V. N. Shastin, M. S. Kuznetsov, S. A. Terentiev, S. A. Nosukhin, D. D. Prikhodko, V. D. Blank, M. Wienold, and H.-W. Hübers, Diamond Relat. Mater. **92**, 259 (2019).